Luminescence properties and charge compensation of $BaMgAl_{10}O_{17}:Mn^{4+}, K^+$ red-emitting phosphor

RENPING CAO*, YUJIAO YE, QIYING PENG, SILING GUO, ZUOFU HU, WEN HU, HUI AO, XIAOGUANG YU
College of Mathematics and Physics, Jinggangshan University, Ji'an 343009, China

$BaMgAl_{10}O_{17}:Mn^{4+}, K^+$ phosphor is synthesized by solid-state method in air. Emission spectrum in the region from 600 to 780 nm is observed with the strong emission peak at ~ 663 nm owing to the $^2E \rightarrow {}^4A_2$ transition of Mn^{4+} ions. Excitation spectrum in the range of 220 - 520 nm monitored at 663 nm is shown with three excitation band peaks ~ 288, 360, and 450 nm. The emission intensity of $BaMgAl_{10}O_{17}:Mn^{4+}$ phosphor is enhanced ~ 1.6 times by co-doping K^+ ion. The luminous mechanism is explained by Tanabe-Sugano diagram of Mn^{4+} ion.

(Received April 26, 2017; accepted February 12, 2018)

Keywords: Phosphors, Mn^{4+} ion, Red-emitting, Charge compensation

1. Introduction

At present, white light-emitting diodes (LEDs) have got extensive development owing to their good marked prospect and excellent properties, such as low power consumptions, high efficiency, and environment friendliness [1,2]. White LEDs have been used as the next generation solid state lighting in many fields, such as lighting, car, traffic signal, mobile phone, and daily life [3,4]. Usually, LED chip-phosphors system is an important method to gain white light. Red-emitting phosphor is one of key luminescent materials in white LEDs based on near ultraviolet (UV) chip, red, green, and blue phosphors. Red phosphor can also improve color rendering index (CRI) and color temperature (CCT) of white LEDs fabricated by using blue LED chip excitation $Y_3Al_5O_{12}:Ce^{3+}$ yellow phosphor [5,6]. Therefore, it is imperative to study novel red-emitting phosphors for white LEDs. The red phosphors doped with Eu^{3+} and Sm^{3+} ions have been reported widely, such as $Ca_2Ga_2SiO_7:Eu^{3+}$, $Ca_2YZr_2Al_3O_{12}:Eu^{3+}$, $NaLa(MoO_4)_2:Sm^{3+}$, and $MgO:Sm^{3+}$ [7-10]. However, their applications are limited owing to the high price of rare earth and the sharp absorption peaks in UV and blue region. Therefore, we choose rare earth free Mn^{4+}-doped phosphors as the research object in the paper.

Mn^{4+} ion (d^3) gives rather complicated optical spectra in different crystalline fields [11]. Absorption spectrum of Mn^{4+} ion covers the whole UV range, and the subsequently emitted luminescence is within the range 600 - 780 nm due to the $^2E \rightarrow {}^4A_2$ transition of Mn^{4+} ion [12]. In 1947, Williams reported the luminescence properties of Mn^{4+} doped magnesium germinate [13]. Subsequently, Kemeny *et al* investigated $3.5MgO{\cdot}0.5MgF_2{\cdot}GeO_2:Mn^{4+}$ red-emitting phosphor in 1960, which is used as commercial red phosphor [14]. However, its applications are limited due to a high price of GeO_2. Over the years, Mn^{4+} doped other phosphors have also been reported widely, such as $La_2LiTaO_6:Mn^{4+}$, $Ca_{14}Zn_6M_{10}O_{35}:Mn^{4+}$ (M = Al^{3+} and Ga^{3+}), $LiNaGe_4O_9:Mn^{4+}$, $Li_2MgTiO_4:Mn^{4+}$, $K_2TiF_6:Mn^{4+}$, $KNaSiF_6:Mn^{4+}$, $Li_2Mg_3SnO_6:Mn^{4+}$, and $Li_2SnO_3:Mn^{4+}$ [15-22]. But their practical applications are not ideal.

The purpose of the work is to research the luminescence properties of $BaMgAl_{10}O_{17}:Mn^{4+}$, K^+ red phosphor for white LEDs. In the paper, a series of $BaMgAl_{10}O_{17}:Mn^{4+}$ and $BaMgAl_{10}O_{17}:Mn^{4+}$, K^+ red phosphors are synthesized by solid-state reaction method in air. The morphologies, crystal structures, luminescence properties, the influence of Mn^{4+} doping concentration, and fluorescence lifetimes are characterized by X-Ray powder diffraction (XRPD), scanning electron microscopy (SEM), and FLS920 spectrofluorimeter, respectively. The charge compensation derived from K^+ ion is investigated. The luminous mechanism is explained by Tanabe-Sugano diagram of Mn^{4+} ion.

2. Experiments

2.1. Raw materials and sample synthesis

$BaMgAl_{10}O_{17}:xMn^{4+}$ (x = 0, 0.2, 0.4, 0.6, 0.8, 1.0, 1.2, 1.4, and 1.6 mol%) and $BaMgAl_{10}O_{17}:1\%Mn^{4+}$, $1\%K^+$ red phosphors are synthesized by solid-state reaction method in air. The stoichiometric amount of raw materials such as $BaCO_3$ (A.R. 99.5%), MgO (A.R. 99.5%), Al_2O_3 (A.R. 99.5%), and $MnCO_3$ (A.R. 99.5%) are well grounded in an agate mortar without further purification, sintered at 600°C for 5 h, grounded again, and subsequently sintered 1400°C for 4 h in air. Repeated grindings are performed between two sintering processes to improve the homogeneity. All products are obtained after natural cooling to room temperature.

2.2. Characterization

The crystal structures of phosphors are checked by XRPD (Philips Model PW1830) with Cu-Kα radiation at 40 kV and 40 mA at room temperature. The data are collected in the 2θ range from 10° to 90°. The morphology of the phosphor is inspected by using SEM (ZEISS, EVO18) operating at an accelerating voltage of 15 kV. Luminescence properties and lifetimes of samples are investigated by using a steady-state FLS920 spectrofluorimeter (Edinburgh Instruments, UK, Edinburgh) with a high spectral resolution (signal to noise ratio > 6000:1) at room temperature.

3. Results and discussions

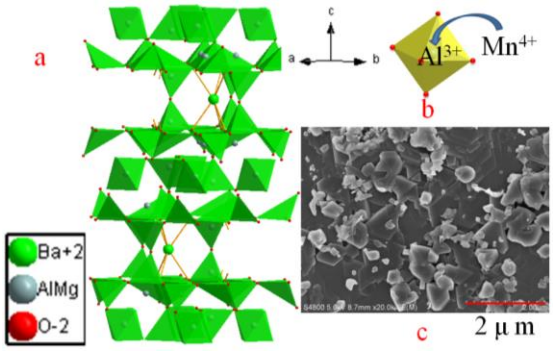

Fig. 1(a). The unit cell of $BaMgAl_{10}O_{17}$ drawn on the basis of ICSD #201727; (b) The polyhedral around central atom Al; (c) SEM image of $BaMgAl_{10}O_{17}$:1%Mn^{4+}, 1%K^{+} phosphor

Fig. 1 shows the unit cell of $BaMgAl_{10}O_{17}$ drawn on the basis of the Inorganic Crystal Structure Database (ICSD) #201727, the polyhedral around central atom Al, and SEM image of $BaMgAl_{10}O_{17}$:1%Mn^{4+}, 1%K^{+} phosphor. $BaMgAl_{10}O_{17}$ is described in the hexagonal crystal system with space-group *p* 63/*mmc* and the lattice parameters a = 5.6275 (7) Å, b = 5.6275 (7) Å, c = 22.658 (70) Å, V = 612.42 $Å^3$, and Z = 4 [23]. The crystal structure of $BaMgAl_{10}O_{17}$ is related to the β-alumina structure of $NaAl_{11}O_{17}$ and exhibits layer structure, which consists of the spinel blocks stacking alternately and the so-called conduction layers containing Ba ions [24,25]. When (Ba, Mg)$^{4+}$ ions replace (Na, Al)$^{4+}$ ions, Ba atoms occupy the mirror plane, and Mg atoms may partially occupy either tetrahedral or octahedral sites of Al atoms in the spinel block to achieve charge compensation of $BaMgAl_{10}O_{17}$ compound [26]. The Mn^{4+} ion occupies the Al^{3+} ion site and the K^{+} ion replaces the Ba^{2+} ion in the host lattice owing to their similar ionic radii (Al^{3+}: ~ 0.535 Å, Mn^{4+}: ~ 0.54 Å, K^{+}: ~ 1.33 Å, and Ba^{2+}: ~ 1.35 Å) [27]. The morphology of $BaMgAl_{10}O_{17}$:1%Mn^{4+}, 1%K^{+} phosphor is flakiness according to the SEM image.

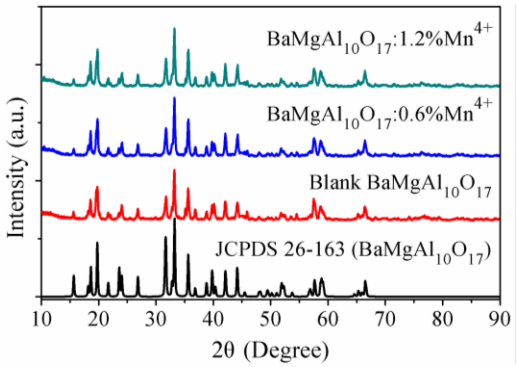

Fig. 2. XRD patterns of JCPDS card no. 26-163 ($BaMgAl_{10}O_{17}$), blank $BaMgAl_{10}O_{17}$, $BaMgAl_{10}O_{17}$:0.6%Mn^{4+}, and $BaMgAl_{10}O_{17}$:1.2%Mn^{4+} phosphors

XRD patterns of Joint Committee on Powder Diffraction Standards (JCPDS) no. 26-163 ($BaMgAl_{10}O_{17}$), blank $BaMgAl_{10}O_{17}$, $BaMgAl_{10}O_{17}$:0.6%Mn^{4+}, and $BaMgAl_{10}O_{17}$:1.2%Mn^{4+} phosphors are shown in Fig. 2. The XRD patterns of these samples match well with the standard data of JCPDS card (no. 26-163). The XRD patterns of other $BaMgAl_{10}O_{17}$:xMn^{4+} ($0 \le x \le 1.6$ mol%) phosphors are not displayed in Fig. 2, but those patterns are also in line with that of JCPDS card (no. 26-163). No other crystalline phase is observed. This is said that all samples are pure phase $BaMgAl_{10}O_{17}$ and doping of Mn^{4+} ions do not cause any significant structure changes due to their similar ionic radii (CN = 6) (Al^{3+}: ~ 0.535 Å and Mn^{4+}: ~ 0.54 Å).

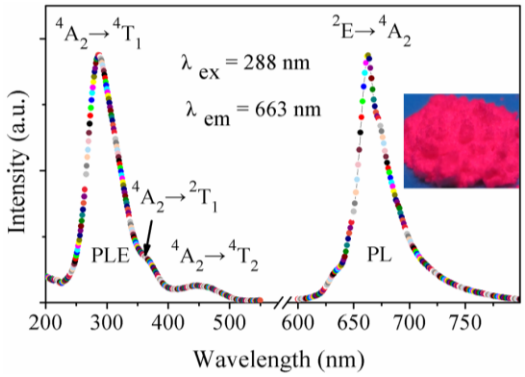

Fig. 3. PL and PLE spectra of $BaMgAl_{10}O_{17}$:1%Mn^{4+} phosphor at room temperature (λ_{ex} = 288 nm and λ_{em} = 663 nm). The inset: Picture of $BaMgAl_{10}O_{17}$:1%Mn^{4+} phosphor under 365 nm UV lamp

Fig. 3 shows photoluminescence (PL) and photoluminescence excitation (PLE) spectra of $BaMgAl_{10}O_{17}$:1%Mn^{4+} phosphor at room temperature (λ_{ex} = 288 nm and λ_{em} = 663 nm) and the picture of $BaMgAl_{10}O_{17}$:1%Mn^{4+} phosphor under 365 nm lamp. $BaMgAl_{10}O_{17}$ host does not show emission. So, the emission source of phosphor comes from Mn^{4+} ion. The broad PLE band monitored at 663 nm is observed within the range 220 - 520 nm, which contains three PLE peaks

located at ~ 288, 360, and 450 nm due to the $^4A_2 \rightarrow {}^4T_1$, $^4A_2 \rightarrow {}^2T_1$, and $^4A_2 \rightarrow {}^4T_2$ transitions of Mn^{4+} ion, respectively [28-30]. PL band peaking at ~ 663 nm with excitation 288 nm covers the region from 600 to 780 nm, which is due to the $^2E \rightarrow {}^4A_2$ transition of Mn^{4+} ion, the anti-stokes vibronic sidebands associated with the excited state ^2E of Mn^{4+} ion, and the vibronics transition of Mn^{4+} ion with zero-phonon line, respectively [31,32]. The picture in Fig. 3 also shows that $BaMgAl_{10}O_{17}:1\%Mn^{4+}$ phosphor emits red light under a 365 nm UV lamp.

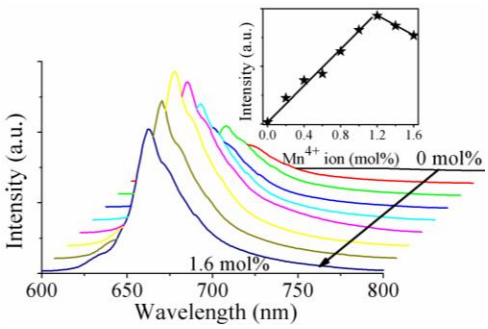

Fig. 4. PL spectra of $BaMgAl_{10}O_{17}:xMn^{4+}$ ($0 \le x \le 1.6$ mol%) phosphors at room temperature (λ_{ex} = 288 nm). The inset: The relation between PL intensity and Mn^{4+} ion concentration

PL spectra of $BaMgAl_{10}O_{17}:xMn^{4+}$ ($0 \le x \le 1.6$ mol%) phosphors at room temperature (λ_{ex} = 288 nm) and the relation between PL intensity and Mn^{4+} ion concentration are shown in Fig. 4. PL spectra shapes and peak positions of $BaMgAl_{10}O_{17}:xMn^{4+}$ ($0.2 \le x \le 1.6$ mol%) phosphors are the same except PL intensity with changing Mn^{4+} ion concentration. The PL intensity increases with increasing Mn^{4+} ion concentration in the range of 0.2 – 1.2 mol% and decreases with the further increasing Mn^{4+} ion concentration. The former observation could be attributed to the distance between Mn^{4+} ions, and the intensity is proportional to the content of Mn^{4+} ion. The latter observation is presumably due to the concentration quenching of Mn^{4+} ions. Therefore, the optimal Mn^{4+} ion concentration is ~ 1.2 mol %.

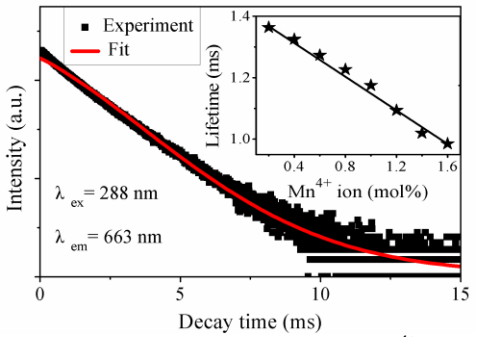

Fig. 5. Decay curve of $BaMgAl_{10}O_{17}:1\%Mn^{4+}$ phosphor at room temperature (The monitoring wavelength is at 663 nm with excitation 288 nm). The red curve is a fit of the experimental data to a first order exponential decay equation. The inset: The relation between lifetime and Mn^{4+} ion concentration

Decay curve of $BaMgAl_{10}O_{17}:1\%Mn^{4+}$ phosphor at room temperature and the relation between lifetime and Mn^{4+} ion concentration are shown in Fig. 5. The monitoring wavelength is at 663 nm with excitation 288 nm. The red curve is a fit of the experimental data to a first order exponential decay equation. The lifetime of $BaMgAl_{10}O_{17}:1\%Mn^{4+}$ phosphor is about 1.16 ms. Lifetime of $BaMgAl_{10}O_{17}:Mn^{4+}$ phosphor decreases from 1.38 to 0.98 ms with increasing Mn^{4+} ion concentration within the range 0.2 - 1.6 mol%. The luminescence decay curve is well fitted by a first-order exponential function [11].

$$I_{(t)} = I_{(0)} \exp(-t/\tau) + A \quad (1)$$

where $I_{(t)}$ is the luminescence intensity at time t, $I_{(0)}$ is the initial luminescence intensity, t is the time, τ is the decay time for the exponential components, and A is the value for different fitting.

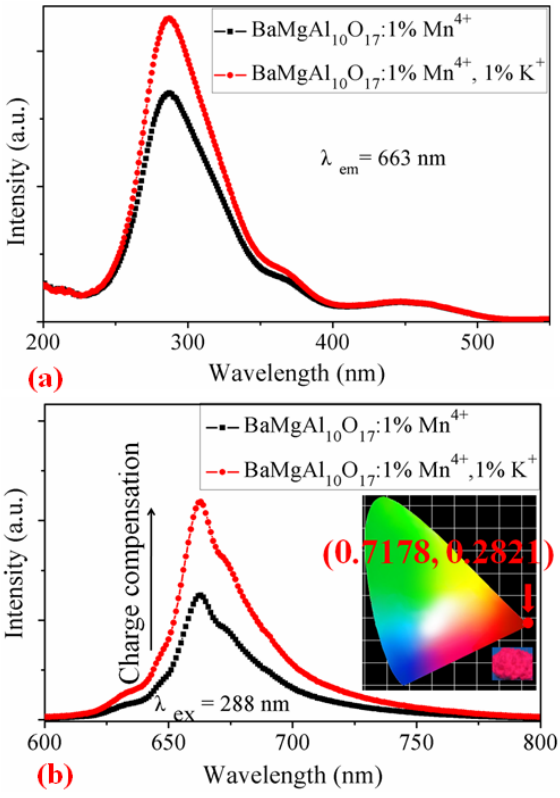

Fig. 6. PLE and PL spectra of $BaMgAl_{10}O_{17}:1\%Mn^{4+}$ and $BaMgAl_{10}O_{17}:1\%Mn^{4+}$, $1\%K^+$ phosphors at room temperature (λ_{ex} = 288 nm). The inset: The chromaticity diagram, chromaticity coordinates, and picture under 365 nm UV lamp

PLE and PL spectra of $BaMgAl_{10}O_{17}:1\%Mn^{4+}$ and $BaMgAl_{10}O_{17}:1\%Mn^{4+}$, $1\%K^+$ phosphors at room temperature (λ_{ex} = 288 nm) are shown in Fig. 6. After Mn^{4+} ion replaces Al^{3+} ion in the host lattice, the charge balance is difficult to keep owing to the different valence state. So, Mn^{4+} ion cannot be fully introduced into the Al^{3+}

ion site in order to keep charge balance. Alkali metal ions (Li^+, Na^+, and K^+) are usually chosen as charge compensator for phosphors due to easy to enter into the lattice, their small ionic radius, and convenient for charge compensation [33]. Here, K^+ ion is selected as charge compensator due to their similar ionic radii (Ba^{3+}: ~ 1.35 Å and K^+: ~ 1.33 Å). PLE and PL intensity of $BaMgAl_{10}O_{17}$:1%Mn^{4+} phosphor is enhanced ~ 1.6 times owing to charge compensation of K^+ ion. The phosphor emits red light and shows satisfying chromaticity coordinate (x = 0.7178, y = 0.2821) under the excitation of 288 nm.

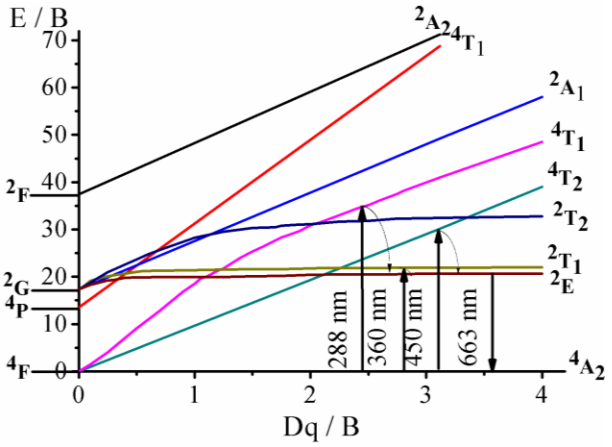

Fig. 7. Tanabe-Sugano diagram of Mn^{4+} ion in octahedral crystal field

Now, we discuss the possible luminous mechanism of Mn^{4+} ion by Tanabe-Sugano diagram of Mn^{4+} ion in octahedral crystal fields shown in Fig. 7. Mn^{4+} (d^3) ion has an incompletely filled *d*-shell, and are not shielded by outer electrons. Its valence state is not stable and can appear and disappear due to irradiation and thermal treatments. Mn^{4+} ion is capable of substituting in a wide variety of metal oxide host systems, e.g., oxygen-coordinated with six nearest neighbors, octahedral, and a distorted octahedral symmetry site etc [11]. The free ion states are ^4F ground level and excited ^2H level. In an octahedral field, the ^4F level splits into the $^4A_2$ ground state and the excited $^4T_2$ and $^4T_1$ states. The spin allowed transitions that could therefore be used to populate the excited states directly correspond to $^4A_2 \rightarrow {}^4T_2$, $^4A_2 \rightarrow {}^2T_1$ (^2H), and $^4A_2 \rightarrow {}^4T_1$ [34]. The emission is assigned to the $^2E \rightarrow {}^4A_2$ transition. The crystal field of host can affect luminescence properties of Mn^{4+} ion.

4. Conclusion

In summary, $BaMgAl_{10}O_{17}$:Mn^{4+} and $BaMgAl_{10}O_{17}$:Mn^{4+}, K^+ red phosphors are synthesized by solid-state reaction method in air. The crystal structures, morphologies, and luminescent properties are investigated. The PL band of $BaMgAl_{10}O_{17}$:Mn^{4+} phosphor covers the region from 600 to 780 nm with the strong PL peak located at ~ 663 nm owing to the $^2E \rightarrow {}^4A_2$ transition of Mn^{4+} ion. The optimal Mn^{4+} ion concentration is ~ 1.2 mol%. The lifetime of $BaMgAl_{10}O_{17}$:1%Mn^{4+} phosphor is ~ 1.16 ms. The lifetimes of $BaMgAl_{10}O_{17}$:xMn^{4+} ($0.2 \le x \le 1.6$ mol%) phosphors decrease from 1.38 to 0.98 ms with increasing Mn^{4+} ion content within the range 0.2 - 1.6 mol%. K^+ ion used as charge compensator can enhance observably the emission intensityof $BaMgAl_{10}O_{17}$:Mn^{4+} phosphor. The luminous mechanism of Mn^{4+} ion is explained by its Tanabe-Sugano diagram. The experiment results indicate that $BaMgAl_{10}O_{17}$:1%Mn^{4+}, 1%K^+ phosphor has application prospect as red phosphor for a UV based white LEDs.

Acknowledgments

This work is financially supported by the National Natural Science Foundation of China (No. 11464021), Natural Science Foundation of Jiangxi Province of China (No. 20171BAB201018), and Foundation of Jiang'xi Educational Committee (No. GJJ160748).

References

[1] N. Zhang, C. Guo, L. Yin, J. Zhang, M. Wu, J. Alloys Compd. **635**, 66 (2015).
[2] Z. Xia, Q. Liu, Prog. Mater Sci. **84**, 59 (2016).
[3] R. Cao, D. Peng, H. Xu, S. Jiang, Z. Luo, H. Ao, P. Liu, J. Lumin. **178**, 388 (2016).
[4] W. Liu, P. Lin, Opt. Express. **22**, A446 (2014).
[5] W. Zhang, Y. Lu, H. Du, J. Lin, J. Long, Ceram. Int. **43**(1), 1080 (2017).
[6] G R. Dillip, G B. Kumar, V. R. Bandi, M. Hareesh, B. D. Prasad Raju, S. W. Joo, L. Krishna Bharat, J. S. Yu, J. Alloys Compd. **699**, 1108 (2017).
[7] G K. Behrh, R. Gautier, C. Latouche, S. Jobic, H. Serier-Brault, Inorg. Chem. **55**(18), 9144 (2016).
[8] X. Wang, Z. Zhao, Q. Wu, Y. Li, Y. Wang, Inorg. Chem. **55**(21), 11072 (2016).
[9] Y. Zhai, W. Zhang, Y. Yin, J. Wang, C. Hu, X. Li, J. Mater. Sci.: Mater. Electron. **27**(9), 9690 (2016).
[10] S. Biju, L. Xu, M. A. H. Alves, R. O. Freirec, Z. Chen, New J. Chem. **41**, 1687 (2017).
[11] G. Blasse, B. C. Grabmaier, Luminescent Materials, Springer-Verlag. Berlin-Heidelberg, 1994.
[12] A. M. Srivastava, W. W. Beers, J. Electrochem. Soc. **143**(9), L203 (1996).
[13] F. E. Williams, J. Opt. Soc. Am. **37**, 302 (1947).
[14] G. Kemeny, C. H. Hakke, J. Chem. Phys. **33**, 783 (1960).
[15] L. Wang, L. Yuan, Y. Xu, R. Zhou, B. Qu, N. Ding, M. Shi, B. Zhang, Y. Chen, Y. Jiang, D. Wang, J. Shi, Appl. Phys. A **117**, 1777 (2014).
[16] K. Seki, K. Uematsu, K. Toda, M. Sato, Chem. Lett. **43**, 1213 (2014).
[17] P. Li, L. Tan, L. Wang, J. Zheng, M. Peng, Y. Wang, J. Am. Ceram. Soc. **99**(6), 2029 (2016).

[18] Y. Lin, Y. Hu, H. Wu, H. Duan, L. Chen, Y. Yu, G. Ju, Z. Mu, M. He, Chem. Eng. J. **288**, 596 (2016).
[19] L. Huang, Y. Zhu, X. Zhang, R. Zou, F. Pan, J. Wang, M. Wu, Chem. Mater. **28**(5), 1495 (2016).
[20] Y. Jin, M. Fang, M. Grinberg, S. Mahlik, T. Lesniewski, M. Brik, G. Luo, J. Lin, R. Liu, ACS Appl. Mater. Interface. **8**, 11194 (2016).
[21] R. Cao, J. Zhang, W. Wang, Z. Hu, T. Chen, Y. Ye, X. Yu, Mater. Res. Bull. **87**, 109 (2017).
[22] R. Cao, W. Wang, J. Zhang, S. Jiang, Z. Chen, W. Li, X. Yu, J. Alloys Compd. **704**, 124 (2017).
[23] N. Iyi, Z. Inoue, S. Kimura, J. Solid State Chem. **61**(2), 236 (1986).
[24] A. F. Wells, Structural Inorganic Chemistry, 5th Edition, Oxford University, New York, 1984.
[25] P. Bollchand, K. C. Mishra, M. Raukas, A. Ellens, P.C. Schmidt, Phys. Rev. B **66**, 134429 (2002).
[26] K. B. Kim, Y. Kim, H. G. Chun, T. Y. Cho, J. S. Jung, J. G. Kang, Chem. Mater. **14**, 5045 (2002).
[27] R. D. Shannon, Acta Cryst. A **32**, 751(1976).
[28] R. Cao, X. Ceng, J. Huang, X. Xia, S. Guo, J. Fu, Ceram. Int. **42**(15), 16817 (2016).
[29] C. Wu, J. Li, H. Xu, J. Wu, J. Zhang, Z. Ci, L. Feng, C. Cao, Z. Zhang, Y. Wang, J. Alloys Compd. **646**, 734 (2015).
[30] Z. Zhou, J. Zheng, R. Shi, N. Zhang, J. Chen, R. Zhang, H. Suo, E. M. Goldys, C. Guo, ACS Appl. Mater. Interfaces. **9**(7), 6177 (2017).
[31] W. Shen, Y. Liu, Z. Wang, Mater. Lett. **161**, 140 (2015).
[32] M. Brik, S. Camardello, A. Srivastava, ECS J. Solid State Sci. Technol. **4**(3), R39 (2015).
[33] R. Cao, Q. Xiong, W. Luo, D. Wu, F. Xiao, X. Yu, Ceram. Int. **41**(5), 7191 (2015).
[34] S. Liang, M. Shang, H. Lian, K. Li, Y. Zhang, J. Lin, J. Mater. Chem. C **5**(11), 2927 (2017).

*Corresponding author: jxcrp@163.com